Left Renal Vein Division during Open Surgical Repair for Abdominal Aortic Aneurysm May Cause Long-Term Kidney Remodeling

吉野, 伸一郎

Left Renal Vein Division during Open Surgical Repair for Abdominal Aortic Aneurysm May Cause Long-Term Kidney Remodeling

Shinichiro Yoshino, Yutaka Matsubara, Shun Kurose, Sho Yamashita, Koichi Morisaki, Tadashi Furuyama, and Tomoharu Yoshizumi, Fukuoka, Japan

Background: Left renal vein division (LRVD) is a maneuver performed during open surgical repair for abdominal aortic aneurysms. Even so, the long-term effects of LRVD on renal remodeling are unknown. Therefore, we hypothesized that interrupting the venous return of the left renal vein might cause renal congestion and fibrotic remodeling of the left kidney.
Methods: We used a murine left renal vein ligation model with 8-week-old to 12-week-old wild-type male mice. Bilateral kidneys and blood samples were harvested postoperatively on days 1, 3, 7, and 14. We assessed the renal function and the pathohistological changes in the left kidneys. In addition, we retrospectively analyzed 174 patients with open surgical repairs between 2006 and 2015 to assess the influence of LRVD on clinical data.
Results: Temporary renal decline with left kidney swelling occurred in a murine left renal vein ligation model. In the pathohistological assessment of the left kidney, macrophage accumulation, necrotic atrophy, and renal fibrosis were observed. In addition, Myofibroblast-like macrophage, which is involved in renal fibrosis, was observed in the left kidney. We also noted that LRVD was associated with temporary renal decline and left kidney swelling. LRVD did not, however, impair renal function in long-term observation. Additionally, the relative cortical thickness of the left kidney in the LRVD group was significantly lower than that of the right kidney. These findings indicated that LRVD was associated with left kidney remodeling.
Conclusions: Venous return interruption of the left renal vein is associated with left kidney remodeling. Furthermore, interruption in the venous return of the left renal vein does not correlate with chronic renal failure. Therefore, we suggest careful follow-up of renal function after LRVD.

INTRODUCTION

Surgical treatment for abdominal aortic aneurysms (AAAs) includes open surgical repair (OSR) and endovascular aneurysm repair. OSR is recommended for younger patients or patients with anatomical conditions that preclude its use, such as those with para/juxta-renal aneurysms.[1−3] Left renal vein division (LRVD) is a maneuver used to gain the sufficient exposure of the proximal

Conflict of interest: The authors declare that they have no competing interests.
Funding sources: The authors have not received any funding.
Declaration of interests: None declared.
Presentation Information: This retrospective clinical study was presented at the 49th Annual Meeting of the Japanese Society for Cardiovascular Surgery, Okayama, Okayama, Japan, on February 11−13, 2019.

Department of Surgery and Science, Graduate School of Medical Sciences, Kyushu University, Fukuoka, Japan.

Correspondence to: Tadashi Furuyama, Department of Surgery and Science, Graduate School of Medical Sciences, Kyushu University, 3-1-1, Maidashi, Higashi-ku, Fukuoka 812-8582, Japan; E-mail: cdq43210@par.odn.ne.jp

Ann Vasc Surg 2023; 96: 155–165
https://doi.org/10.1016/j.avsg.2023.03.035

Manuscript received: January 28, 2023; manuscript accepted: March 30, 2023; published online: 17 April 2023

neck of the abdominal aorta. LRVD is performed in 3.0–22.2% of AAAs.[3–8] The left renal vein has collateral veins; therefore, renal congestion after LRVD is considered a rare or temporary occurrence.[9] Conversely, several reports have indicated that LRVD may result in postoperative congestive renal injury and consequent renal dysfunction.[7,8,10–12] Renal venous hypertension reduces the estimated glomerular filtration rate (eGFR) and causes high renal interstitial hydrostatic pressure. As such, they might result in renal fibrosis with macrophage accumulation.[13–16] However, the morphological and histological effects of LRVD on the kidneys remain unclear. Therefore, morphological and histological assessments of the kidney after LRVD are required.

Animal models were used for histological assessments of the kidneys after left renal vein ligation (LRVL).[13,17] Computed tomography (CT) scans clinically assess postoperative kidney morphology, including kidney volume and renal cortical thickness, which are affected by renal congestion and remodeling.[18–21] The mechanism by which renal congestion affects kidney remodeling is unclear. Even so, macrophages are known to play an important role in organ congestion.[22–26] We previously reported that macrophages play an important role in vascular remodeling.[27,28]

Therefore, in this study, we hypothesized that renal congestion caused by the interrupted venous return of the left renal vein would lead to macrophage accumulation and fibrotic remodeling in the left kidney. We verified the hypothesis using the murine LRVL model. Furthermore, we confirmed the consistency of our results through a comparative analysis of clinical data.

MATERIALS AND METHODS

For detailed methods, see Supplemental Materials.

Study Design and Experimental Approval

All animal experiments were approved by the Animal Care and Use Committee of Kyushu University (Approval no. A20-240-0). All animals were handled as per the National Research Council's Guide for the Care and Use of Laboratory Animals. This clinical retrospective study was approved by the Institutional Review Board of Kyushu University (Approval No. 30-538). The study was performed in accordance with the principles of the Declaration of Helsinki. Although a written informed consent was waived due to the retrospective nature of the study, patients were informed of their right to opt out of the study.

Murine Left Renal Vein Ligation Model

Wild-type male C57BL6/J mice, aged 8–12 weeks, were used in this study. Detailed procedures are documented in the Supplemental Materials. Briefly, under general anesthesia, the left renal vein (LRV) was ligated with a 7-0 silk suture under a microscope while preserving the branches of the LRV (Supplemental Fig. S1), as previously described.[17] Blood samples and bilateral kidneys were collected from various mice prior to the procedure as a preoperative baseline and on days 1, 3, 7, and 14 following LRVL. After laparotomy under general anesthesia, blood samples were collected from the inferior vena cava with a 27-gauge needle puncture before perfusion fixation; subsequently, bilateral kidneys were harvested.

Histology

Perfusion fixation with 10% formalin via the left ventricle under physiological pressure was performed for bilateral kidney extractions. The kidneys were fixed in 10% formalin for 24 hr, embedded in paraffin, and cut into 4-μm cross-sections. Hematoxylin-eosin (HE) and Sirius red staining were performed for histological assessment. Cell counts in 10 random high-power fields (HPFs) around the renal cortex were performed in each cross-section and averaged. Cells were identified on HE-stained slides, and renal fibrosis was assessed on Sirius red-stained slides. Sirius red-stained areas were manually traced and measured using the color thresholding of the ImageJ software (http://imagej.nih.gov/ij/). Ten random HPFs around the renal cortex were evaluated in each section; the values were averaged. Additional unstained cross-sections from the same regions were used for immunohistochemistry and immunofluorescence microscopy.

Immunohistochemistry

As previously described, immunohistochemical staining for TNF-α, IL-1β, and TGF-β1 was performed on 4-μm formalin-fixed and paraffin-embedded sections.[29] Detailed methods and all primary and secondary antibodies are listed in the Supplemental Materials.

Immunofluorescence

Immunofluorescence for CD68, TNF-α, iNOS, Arginase-1, mannose receptor, and αSMA was performed on the 4-μm formalin-fixed and paraffin-

embedded sections, as previously described.[30] Detailed methods and all primary and secondary antibodies are listed in the Supplemental Materials. The sections were observed under a fluorescence microscope (Biorevo BZ-90000; Keyence, Osaka, Japan).

RNA Extraction and Real-Time Quantitative Polymerase Chain Reaction

Total RNA was isolated from kidney samples and converted into cDNA for real-time polymerase chain reaction analysis using a TaqMan Gene Expression Assay probe and primer mix, as previously described.[31] Relative mRNA expressions of TNF-α, IL-1β, TGFβ1, and GAPDH were determined by the $\Delta\Delta$Ct method, based on the relative expression of the target gene compared to a reference gene (GAPDH) and normalized to the control samples. The detailed methods and primers are listed in the Supplemental Materials.

Patients

We conducted a retrospective study of patients who underwent elective OSR for AAA between January 2006 and December 2016 at the Department of Surgery and Science, Kyushu University Hospital, Fukuoka, Japan. Clinical characteristics, anatomical information for the AAAs, and operative records were retrieved from medical records. Patients' eGFRs were calculated as per the Japanese equation: $\text{eGFR} = 194 \times \text{serum creatinine}^{-1.094} \times \text{age}^{-0.287} \times 0.739$ [if female].[32]

Surgical Procedures and Outcomes

An individual surgeon decided to perform LRVD to expose the perirenal aorta intraoperatively. The LRV was divided close to the inferior vena cava to preserve the collateral venous drainage of the LRV.

Changes in relative eGFR, relative kidney volume, and relative cortical thickness were assessed and compared to the preoperative values after OSR. Acute kidney injury was defined as a $>$ 2.0-fold increase in serum creatinine concentration or a $>$ 50% decrease in eGFR compared to baseline, as previously described.[31,33] Kidney length, lateral and anterior-posterior diameters, and cortical thickness were measured using CT scan. Kidney volume was calculated using the ellipsoid formula (volume = length $\times$ lateral diameter $\times$ anterior-posterior diameter $\times$ $\pi/6$) as previously described.[18] The time points for evaluating the eGFR and left kidney volume were preoperative, in the acute postoperative phase (approximately 7 days after surgery), and in the chronic phase (1 year or more after surgery). In addition, cortical thickness was assessed as a surrogate marker of kidney remodeling.[19–21] The cortical thickness was measured perpendicular to the capsule in a sagittal cross-sectional view of a contrast image at 3 different locations in each patient, modifying a previously described method;[19–21] the average value for 3 points was considered the patient's cortical thickness. After surgery, patients were followed up with blood tests and CT scans. The relative eGFR, relative kidney volume, and relative cortical thickness at each time point were calculated with a preoperative value of 100%.

Statistics

Data are presented as mean ± standard deviation. First, normality was confirmed using the Shapiro–Wilk test. Then, statistical significance was determined using the Student's *t*-test, Wilcoxon rank sum test, or analysis of variance (ANOVA), followed by Dunnett's or Sidak's post hoc correction. Finally, the statistical significance was set at $P < 0.05$. All data were analyzed using JMP Pro 15.0.0 software (SAS Institute Inc., Cary, North Carolina).

RESULTS

The Murine Left Renal Vein Ligation Model Showed a Temporary Increase in Blood Urea, Nitrogen, and Creatinine with Kidney Swelling

We assessed renal function and kidney weight in the murine LRVL model. Serum blood urea, nitrogen, and creatinine concentrations peaked 1 day after LRVL and then decreased (Fig. 1A and B). After LRVL, the weight of the left kidney significantly increased on postoperative days 1, 3, and 7 than the preoperative weights of the left kidney. In contrast, there was no significant change in the right kidney weight on day 1. The right kidney became gradually enlarged on days 3, 7, and 14 (Fig. 1C–E). These results showed that LRVL might be associated with renal congestion and a temporary decrease in renal function in the murine LRVL model.

Mouse Left Renal Vein Ligation Causes Kidney Congestion, Reduced Numbers of Renal Tubules and Glomeruli, and an Accumulation of Inflammatory Cells

The pathological effects of LRVL on the left kidney were microscopically examined. HE stains showed blood congestion within the kidney 1 day after LRVL and washout of red blood cells 3 days after

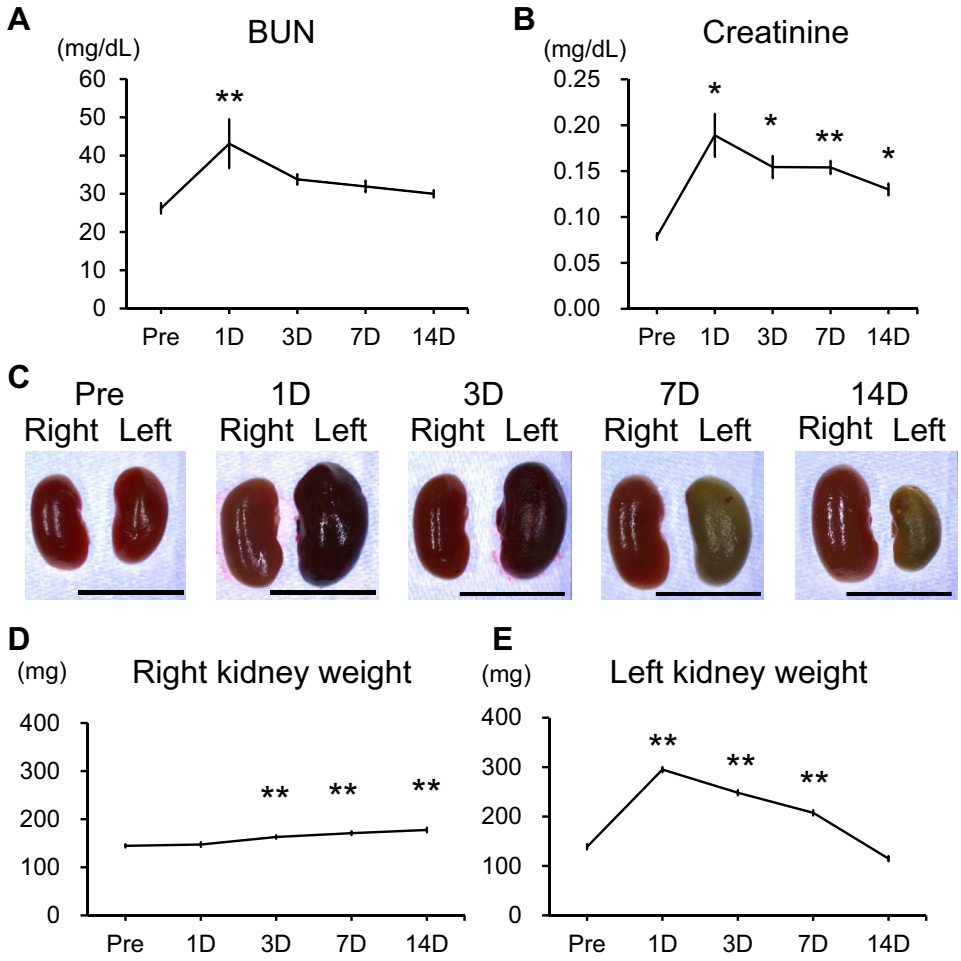

Fig. 1. (A) Line graph showing serum blood urea nitrogen concentrations before and 1, 3, 7, and 14 days after *left* renal vein ligation (LRVL) in 8−10 mice. Plotted values represent means. Bars indicate the standard deviation (SD) [$P = 0.006$ (ANOVA). $^{**}P < 0.01$ (after post hoc correction)]. **(B)** Line graph showing serum creatinine concentrations before and 1, 3, 7, and 14 days after LRVL in 8−10 mice. Plotted values represent means. Bars indicate SD [$P < 0.001$ (ANOVA); $^{*}P < 0.05$ and $^{**}P < 0.01$ (after post hoc correction)]. **(C)** Macroscopic images of the *right* and *left* kidneys of mice after LRVL. Scale bar, 10.0 mm. **(D)** Line graph showing the *right* kidney weights before and 1, 3, 7, and 14 days after LRVL in 10−13 mice. Plotted values represent means. Bars indicate SD. $P < 0.001$ (ANOVA). $^{**}P < 0.01$ (after post hoc correction). **(E)** A line graph showing *left* kidney weights before and 1, 3, 7, and 14 days after LRVL in 10−13 mice. Plotted values represent means. Bars indicate SD [$P < 0.001$ (ANOVA). $^{**}P < 0.01$ (after post hoc correction)].

LRVL (Fig. 2A and B). In addition, the number of living renal tubules and glomeruli progressively decreased over the first 14 days after LRVL (Fig. 2A, C, and D). These findings indicate that LRVL may damage kidney cells associated with remodeling. Since inflammatory cells such as macrophages play an important role in kidney remodeling after AKI and chronic kidney disease,[16,34] we quantified the number of mononuclear inflammatory cells in the left kidney after LRVL. The number of mononuclear cells progressively increased over the first 14 days after LRVL, indicating macrophage accumulation in the remodeled kidneys (Fig. 2A and E). In summary, LRVL caused kidney congestion followed by macrophage accumulation and a reduction in the number of tubules and glomeruli. LRVL may, therefore, be associated with kidney remodeling.

Mouse Left Renal Vein Ligation Caused Renal Fibrosis with Myofibroblast-Like Macrophage Accumulation

Renal fibrosis was evaluated to confirm kidney remodeling after mouse LRVL. This evaluation was

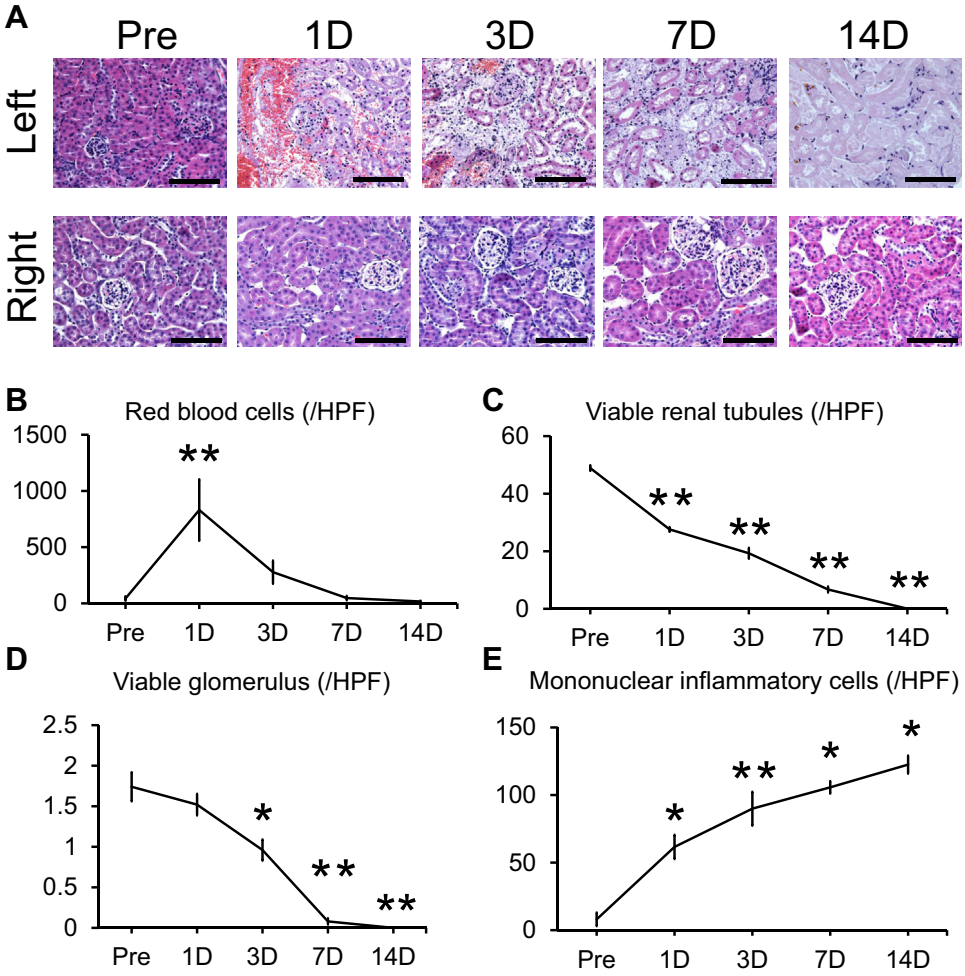

Fig. 2. **(A)** Representative microscopic images of hematoxylin and eosin-stained *right* and *left* mouse kidney cortex tissues following *left* renal vein ligation (LRVL). Scale bar, 100 μm. **(B)** Line graph showing the number of red blood cells per high-power field (HPF). Five mice were examined before and 1, 3, 7, and 14 days after LRVL. The plotted values represent the mean values, while the bars indicate the standard deviation (SD) [$P = 0.001$ (ANOVA); $^{**}P < 0.01$ (after post hoc correction)]. **(C)** Line graph showing the number of viable renal tubules per HPF. Five mice were examined in total. The plotted values represent the mean values, while the bars indicate the SD [$P < 0.001$ (ANOVA); $^{**}P < 0.01$ (after post hoc correction)]. **(D)** Line graph showing the number of viable glomeruli per HPF. Five mice were examined in total. The plotted values represent the mean values, while the bars indicate the SD [$P < 0.001$ (ANOVA). $^{**}P < 0.01$ (after post hoc correction)]. **(E)** Line graph showing the number of mononuclear inflammatory cells per HPF. Five mice were examined in total. The plotted values represent the mean values, while the bars indicate the SD [$P < 0.001$ (ANOVA); $^{**}P < 0.01$ (after post hoc correction)].

based on the fact that renal fibrosis plays an important role in the decline of renal function and the progression of chronic kidney disease.[35] Areas stained by Sirius red in the mouse kidney sections indicated renal fibrosis. Although there was little fibrosis in the right kidney after LRVL (Fig. 3A and B), fibrosis was observed in the left kidney on days 7 and 14 after LRVL (Fig. 3A and C), indicating that LRVL induced fibrosis only in the left kidney. Since macrophage accumulation was observed in the left kidney after LRVL and myofibroblast-like macrophages are associated with renal fibrosis,[36] we performed immunofluorescence staining for CD68 + α-SMA + cells to confirm myofibroblast-like macrophages. Myofibroblast-like macrophages were not confirmed in the right kidney after LRVL; however, a significant accumulation of myofibroblast-like macrophages was observed in the left kidney (Fig. 3D and E). In summary, LRVL causes renal fibrosis, which is associated with

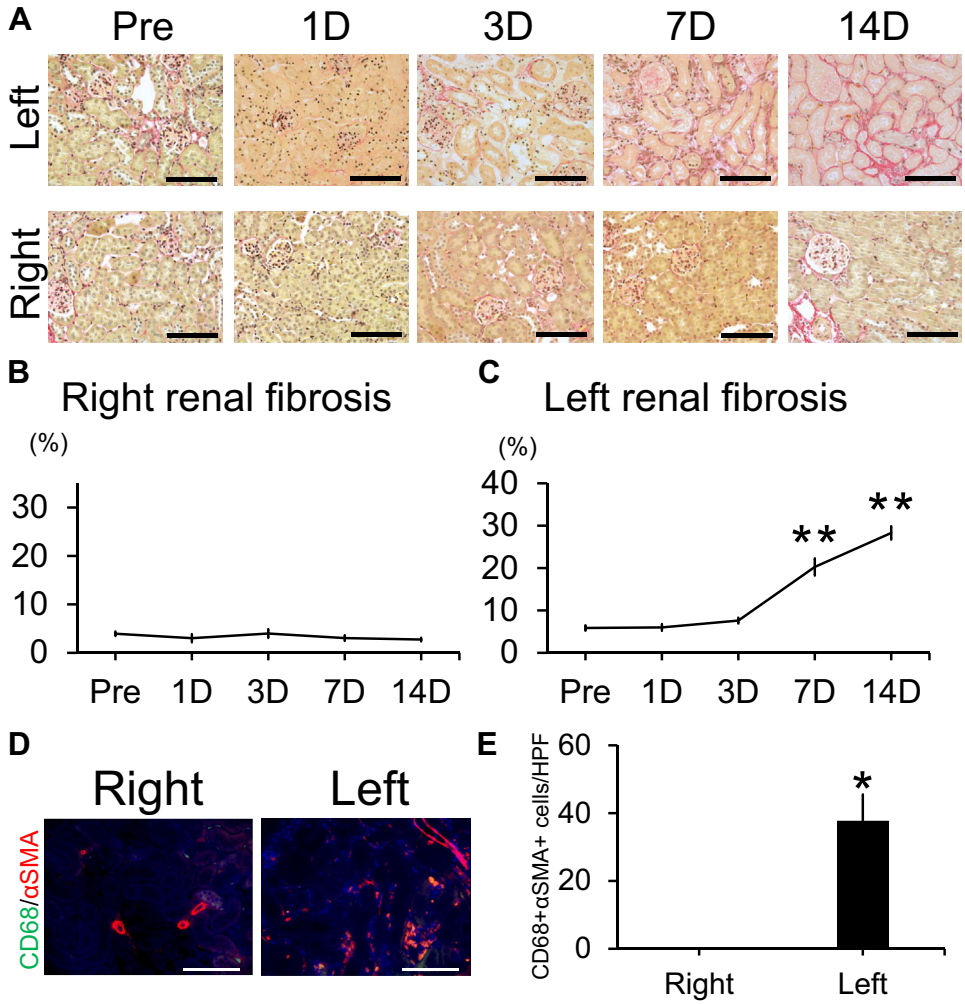

Fig. 3. (A) Representative microscopic images of Sirius red staining of the *right* and *left* kidneys after *left* renal vein ligation (LRVL) in mice. Scale bar, 100 μm. **(B)** A line graph shows the quantitative area of fibrosis (%) in the *right* kidney before and 1, 3, 7, and 14 days after LRVL. Five mice were examined. Plotted values represent means. Bars indicate the standard deviation (SD) [$P = 0.55$ (ANOVA)]. **(C)** Line graph showing the quantitative area of fibrosis (%) in the *left* kidney before and 1, 3, 7, and 14 days after LRVL. Five mice were examined. Plotted values represent means. Bars indicate SD [$P < 0.001$ (ANOVA). $^{**}P < 0.01$ (after post hoc correction)]. **(D)** Representative microscopic images of immunofluorescent staining for CD68 (green) and α-SMA (red) in the *right* and *left* kidneys 14 days after LRVL. Scale bar, 100 μm. **(E)** Bar graphs showing the number of CD68 + α-SMA + cells per high-power field in the *right* and *left* kidneys after LRVL. Four mice were examined. Plotted values represent means. Bars indicate SD [$^{*}P < 0.05$ (Wilcoxon rank sum test)].

myofibroblast-like macrophage accumulation in the left kidney.

M1 and M2 Macrophage Accumulation in the Left Kidney after Mouse Left Renal Vein Ligation is Concomitant with the Expression of TNF-α, IL-1β, and TGF-β1

Although myofibroblast-like macrophage accumulation increased in the left kidney after mouse LRVL, which might be associated with renal fibrosis, macrophage polarization after mouse LRVL was assessed. Immunofluorescence staining was performed on CD68 + iNOS (inducible nitric oxide synthase) + cells (M1 macrophages), CD68+TNF-α (tumor necrosis factor alpha) + cells (M1 macrophages), CD68 + Arg-1 (arginase-1) + cells (M2 macrophages), and CD68 + MR (mannose receptor) + cells (M2 macrophages) (Fig. 4A). The accumulations of both M1 macrophages (Fig. 4A–C) and M2

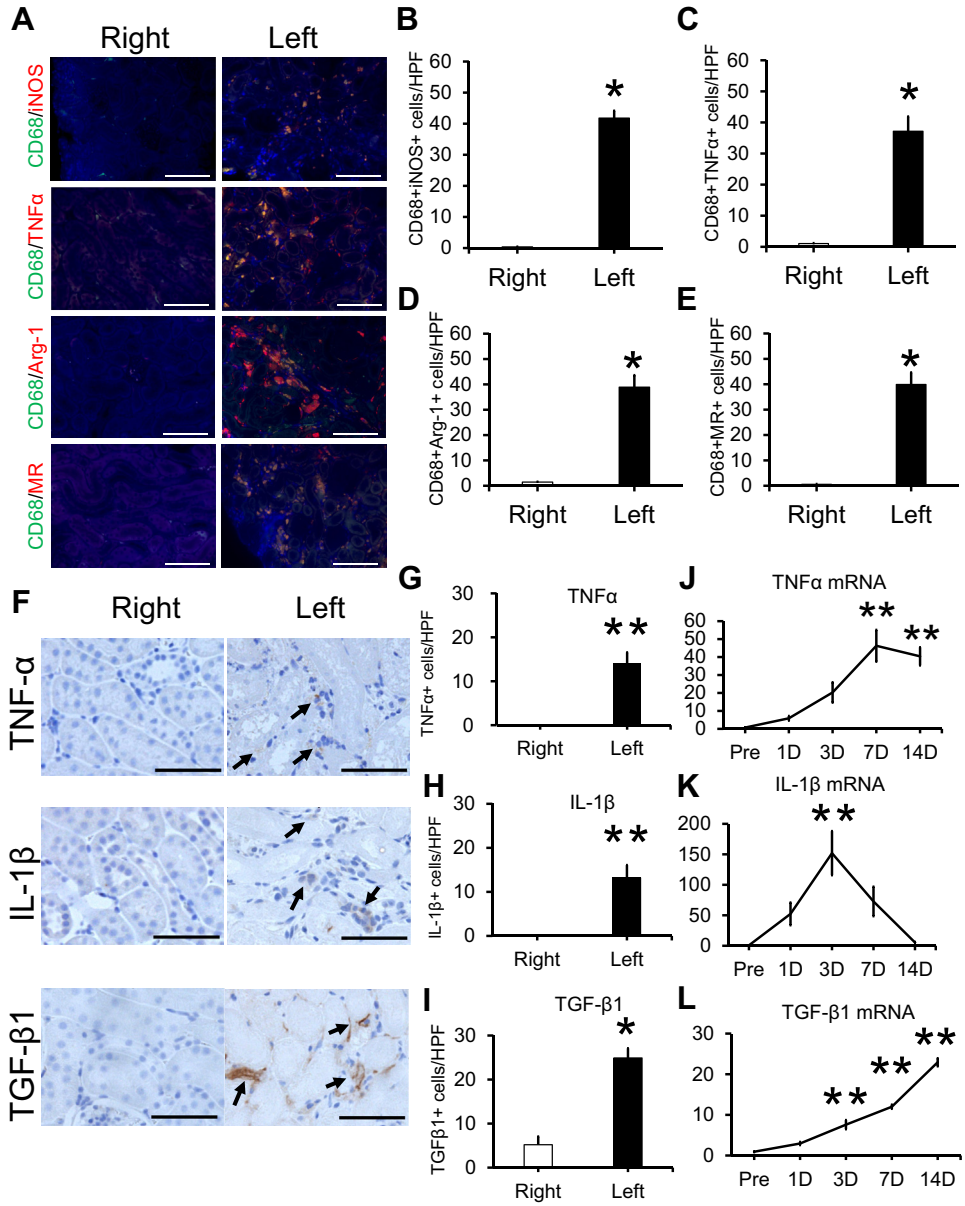

Fig. 4. **(A)** Representative microscopic images of immunofluorescent staining for CD68+ (green) and iNOS+ (red), CD68+ (green) and TNF-α+ (red), CD68+ (green) and arginase-1 (Arg-1)+ (red), or CD68+ (green) and mannose receptor (MR)+ (red) cells in the *right* and *left* kidneys 14 days after *left* renal vein ligation (LRVL) in mice. Scale bar, 100 μm. **(B)** Bar graphs showing the number of CD68 + iNOS + cells per high-power field (HPF) in the *right* and *left* kidneys after LRVL. Four mice were examined. Plotted values represent means. Bars indicate standard deviation (SD) [$*P < 0.05$ (Wilcoxon rank sum test)]. **(C)** Bar graphs showing the number of CD68 + TNF-α + cells per HPF in the *right* and *left* kidneys after LRVL. Four mice were examined. Plotted values represent means. Bars indicate SD [$*P < 0.05$ (Wilcoxon rank sum test)]. **(D)** Bar graphs showing the number of CD68 + Arg-1 + cells per HPF in the *right* and *left* kidneys after LRVL. Four mice were examined. Plotted values represent means. Bars indicate SD [$*P < 0.05$ (Wilcoxon rank sum test)]. **(E)** Bar graphs showing the number of CD68 + MR + cells per HPF in the *right* and *left* kidneys after LRVL. Four mice were examined. Plotted values represent means. Bars indicate SD [$*P < 0.05$ (Wilcoxon rank sum test)]. **(F)** Representative microscopic images of immunohistochemical staining for TNF-α+, IL-1β, and TGF-β1 in the *right* and *left* kidneys 14 days after mouse LRVL. Scale bar, 50 μm. **(G)** Bar graphs showing the number of TNF-α + cells per HPF in the *right* and *left* kidneys. Five mice were examined. Plotted values represent means. Bars indicate SD [$**P < 0.01$ (Wilcoxon rank sum test)]. **(H)** Bar graphs showing the number of IL-1β + cells per HPF in the *right* and *left* kidneys. Five mice were examined. Plotted values represent means. Bars indicate SD

macrophages (Fig. 4A, D, and E) were significantly higher in the left kidney than in the right kidney after LRVL. TNF-α, IL-1β, and TGF-β play important roles in renal fibrosis and are produced by both M1 and M2 macrophages;[28,37,38] therefore, immunohistochemical staining was performed for identifying these cytokines after LRVL. All of these cytokines increased in the left kidney after LRVL (Fig. 4F–I). Quantitative polymerase chain reaction was also performed to assess the mRNA expression of these cytokines. As expected, the mRNA expression for all 3 genes was increased in the left kidney after LRVL (Fig. 4J–L). These findings indicate that M1 and M2 macrophages are associated with increased TNF-α, IL-1β, and TGF-β production, which may cause renal fibrosis after LRVL.

Patients Who Underwent Left Renal Vein Division Experienced a Temporary Renal Decline with Kidney Swelling, Followed by a Reduction in the Cortex Thickness of the Left Kidney

One hundred and seventy four patients were included in the study. LRVD was performed on 26 patients. Table I shows the patient characteristics and postoperative clinical outcomes. The non-LRVD and LRVD groups significantly differed in operation times (286 vs. 380 min, $P < 0.01$), the proportion of patients with cerebrovascular disease (15.5% vs. 46.2%, $P < 0.01$), and the proportion of patients who had suprarenal or inter-renal artery clamps (11.5% vs. 65.4%, $P < 0.01$). Acute kidney injury (AKI) occurred in 13 patients in all cohorts, and all instances of AKI occurred within 2 postoperative days. The incidence of AKI was significantly higher in the LRVD group than in the non-LRVD group (38.5% vs. 2.0%, $P < 0.01$). Supplementary Figure S2A shows the relative eGFR for each group before and after surgery. The postoperative relative eGFR in the acute phase was significantly lower in the LRVD group. However, the differences in relative eGFR at 1, 3, and 5 years between the groups were insignificant. Morphologically, the relative left kidney volume significantly increased in the acute phase after surgery (Supplementary Fig. S2B) and gradually decreased over time. These findings were consistent with the mouse LRVD model.

We also assessed the renal cortical thickness, which was affected by renal remodeling. The relative reduction in renal cortical thickness was more significant in the left kidney than in the right kidney (83.8% vs. 93.3%, $P < 0.05$; Supplementary Fig. S2C). In summary, these findings indicate that LRVD is associated with temporary reductions in eGFR, temporary left kidney swelling, and decreased cortical thickness in the left kidney. Therefore, LRVD does not cause chronic renal decline but may cause renal remodeling.

DISCUSSION

This study showed that murine LRVL caused temporary renal dysfunction accompanied by renal swelling (Fig. 1A–E). In addition, histopathological assessment of the left kidney after LRVL demonstrated significant renal congestion (Fig. 2A–B), followed by macrophage accumulation (Fig. 4A–E), increased inflammatory cytokines (Fig. 4F–L), renal atrophy (Fig. 1C and E), and renal fibrosis (Fig. 3A–C). These findings indicate that an interruption of the venous return caused by LRVL may lead to temporary congestive renal decline followed by left kidney remodeling. In addition, patients with LRVD showed temporary renal dysfunction, left kidney swelling, and reduced left kidney cortex thickness. These findings indicate that LRVD is associated with temporary congestive renal decline followed by left kidney remodeling, similar to the mouse LRVL model.

Renal venous hypertension reduces the GFR[15,39] and increases the renal interstitial pressure associated with fibrotic remodeling.[15] In this study, we showed renal congestion and renal fibrosis after LRVL (Fig. 1A–C, 2A–E, and 3A–C). These findings indicate that venous hypertension after a venous return interruption of the LRV increases the renal

[$^{**}P < 0.01$ (Wilcoxon rank sum test)]. **(I)** Bar graphs showing the number of TGF-β1 + cells per HPF in the *right* and *left* kidneys. Five mice were examined. Plotted values represent means. Bars indicate SD [$^{*}P < 0.05$ (Wilcoxon rank sum test)]. **(J)** Line graph showing the relative mRNA expression levels of TNF-α. Values were normalized to those prior to LRVL. Five mice were examined. Plotted values represent means. Bars indicate SD [$P < 0.001$ (ANOVA) $^{**}P < 0.01$ (after post hoc correction)]. **(K)** Line graph showing the relative mRNA expression levels of IL-1β. Values were normalized to those prior to LRVL. Five mice were examined. Plotted values represent means. Bars indicate SD [$P < 0.001$ (ANOVA). $^{**}P < 0.01$ (after post hoc correction)]. **(L)** Line graph showing the relative mRNA expression levels of TGF-β1. Values were normalized to those prior to LRVL. Five mice were examined. Plotted values represent means. Bars indicate SD [$P < 0.001$ (ANOVA). $^{**}P < 0.01$ (after post hoc correction)].

Table I. Patient characteristics with or without LRVD

Variables	Non-LRVD $N = 148$	LRVD $N = 26$	P value
Age, years	72.1 ± 8.8	74.3 ± 9.0	0.22[a]
Male	127 (85.8)	22 (84.6)	0.77[b]
Hypertension	123 (83.1)	21 (80.8)	0.78[b]
Diabetes mellitus	17 (11.5)	3 (11.5)	1.00[b]
Dyslipidemia	54 (36.5)	9 (34.6)	1.00[b]
Chronic kidney disease	71 (48.0)	14 (53.9)	0.67[b]
Preoperative creatinine level, mg/dL	1.01 ± 0.40	1.03 ± 0.41	0.81[a]
Preoperative eGFR, mL/min/1.73 m^2	61.0 ± 20.3	59.7 ± 20.3	0.75[a]
Aneurysm diameter, mm	53.3 ± 12.2	54.8 ± 9.3	0.55[a]
Juxta-/Pararenal aneurysm	14 (9.5)	15 (57.7)	<0.01[b]
Supra- or inter-renal artery clamp	17 (11.5)	17 (65.4)	<0.01[b]
Operation time, min	286 ± 106	380 ± 92	<0.01[a]
Blood loss, mL	1,692 ± 1,677	2,161 ± 1,263	0.18[a]
Renal ischemic time, min	56.9 ± 19.8	63.5 ± 37.9	0.45[a]
Reconstruction of renal artery	2 (1.4)	1 (3.9)	0.39[b]
Cold lactated ringer's solution	2 (1.4)	1 (3.9)	0.39[b]
AKI	3 (2.0)	10 (38.5)	<0.01[b]
Day of AKI occurrence			0.03[b]
1 POD	0 (0.0)	7 (70.0)	
2 POD	3 (100.0)	3 (30.0)	

Data are presented as means ± standard deviation or numbers (%).
eGFR, estimated glomerular filtration rate; AKI, acute kidney injury; POD, postoperative day.
[a]Student's *t*-test.
[b]Fisher's exact test.

interstitial pressure, causing tubular necrosis, glomerular necrosis, and renal fibrosis. In congestive organ damage, such as pulmonary or hepatic congestion, macrophages are considered an important factor.[22–26] For this reason, we focused on macrophages as a mechanism of fibrotic renal remodeling after LRVL.

Fibrosis is a repair process that occurs after tissue inflammation. However, fibrosis that occurs progressively or excessively causes organ dysfunction.[35,38] Macrophages are cells of the innate immune system and are classically divided into M1 and M2 phenotypes. M1 macrophages have proinflammatory properties and secrete inflammatory cytokines, which can cause tissue injury. On the other hand, M2 macrophages have anti-inflammatory properties and secrete anti-inflammatory cytokines that remodel the repair process.[26,28,37] In relation to macrophages, myofibroblasts also have an important role in the fibrotic repair process. A previous study showed that CD68 + αSMA + myofibroblast-like macrophages play an important role in renal fibrosis.[36] In this study, we also showed that renal fibrosis after LRVL is accompanied by an accumulation of M1, M2, and CD68 + αSMA + macrophages (Fig. 3D–E). Furthermore, we showed that M1 and M2 macrophages accumulate with TNF-α, IL-1β, and TGF-β1 in mouse kidneys after LRVL (Fig. 4F–L). These results indicate that macrophages and their cytokines are associated with renal fibrosis after LRVL.

In clinical practice, LRVD is associated with a higher incidence of postoperative AKI (Table I and Supplementary Fig. S2A) and temporary left kidney swelling (Supplementary Fig. S2B); however, long-term kidney function was similar between the patients with and without LRVD. These findings support previous reports that have shown that LRVD can be safely performed.[9]

We also assessed the renal cortical thickness after LRVD because a reduction in renal cortical thickness is associated with chronic kidney disease and is affected by renal remodeling.[19–21] We found a reduction in renal cortical thickness in patients with LRVD (Supplementary Fig. S2C). This finding indicates that LRVD may cause left kidney remodeling. These findings were similar to those of the mouse LRVL model. Although pathological analysis of the left kidney was not performed in human patients, left kidney fibrosis might occur after LRVD. Therefore, left kidney remodeling should be carefully followed up in patients with LRVD.

Limitations

Our study had a few limitations. First, the clinical portion of the study was retrospective in design;

thus, biases in the renal outcome data were observed. Second, the number of patients who underwent LRVD or developed postoperative AKI was small. This may have introduced a type II error. Third, the following limitations of the murine LRVL model should be considered: (1) We used wild-type C57BL/6 mice that do not reflect an ''AAA'' model; (2) Some differences were evident in the venous anatomy between C57BL/6 mice and humans;[40] and (3) We only used 8–12-week-old wild-type male mice in the LRVL model, which may not completely represent the human anatomy.

CONCLUSION

Interruption of the venous return of the left renal vein (LRVL and LRVD) is associated with a temporary decline in renal function accompanied by renal congestion in the left kidney. In addition, LRVD may cause left kidney remodeling, characterized by renal fibrosis accompanied by macrophage accumulation. Further research on the risk of AKI and left kidney remodeling after LRVD is warranted to identify the potential risks of LRVD on kidney remodeling.

We would like to thank Editage (www.editage.com) for English language editing.

SUPPLEMENTARY DATA

Supplementary data to this article can be found online at https://doi.org/10.1016/j.avsg.2023.03.035.

REFERENCES

1. Dansey KD, Varkevisser RRB, Swerdlow NJ, et al. Epidemiology of endovascular and open repair for abdominal aortic aneurysms in the United States from 2004 to 2015 and implications for screening. J Vasc Surg 2021;74:414–24.
2. Patel R, Sweeting MJ, Powell JT, et al. Endovascular versus open repair of abdominal aortic aneurysm in 15-years' follow-up of the UK endovascular aneurysm repair trial 1 (EVAR trial 1): a randomised controlled trial. Lancet 2016;388:2366–74.
3. Wanhainen A, Verzini F, van Herzeele I, et al. Editor's choice e European Society for Vascular Surgery (ESVS) 2019 clinical practice guidelines on the management of abdominal aorto-iliac artery aneurysms. Eur J Vasc Endovasc Surg 2019;57:8–93.
4. Sugimoto M, Takahashi N, Niimi K, et al. Long-term fate of renal function after open surgery for juxtarenal and pararenal aortic aneurysm. J Vasc Surg 2018;67:1042–50.
5. Wang L, Xin SJ, Song Z, et al. Left renal vein division during open surgery of abdominal aortic disease: a propensity score-matched case-control study. Eur J Vasc Endovasc Surg 2013;46:227–31.
6. Komori K, Furuyama T, Maehara Y. Renal artery clamping and left renal vein division during abdominal aortic aneurysm repair. Eur J Vasc Endovasc Surg 2004;27:80–3.
7. Huber D, Harris JP, Walker PJ, et al. Does division of the left renal vein during aortic surgery adversely affect renal function? Ann Vasc Surg 1991;5:74–9.
8. West CA, Noel AA, Bower TC, et al. Factors affecting outcomes of open surgical repair of pararenal aortic aneurysms: a 10-year experience. J Vasc Surg 2006;43:921–7.
9. Samson RH, Lepore MR Jr, Showalter DP, et al. Long-term safety of left renal vein division and ligation to expedite complex abdominal aortic surgery. J Vasc Surg 2009;50:500–4.
10. Dubois L, Durant C, Harrington DM, et al. Technical factors are strongest predictors of postoperative renal dysfunction after open transperitoneal juxtarenal abdominal aortic aneurysm repair. J Vasc Surg 2013;57:648–54.
11. Chung BH, Kang JH, Heo SH, et al. The effect of left renal vein division on renal function following open abdominal aortic surgery using propensity score matching analysis. Ann Vasc Surg 2020;62:232–7.
12. AbuRahma AF, Robinson PA, Boland JP, et al. The risk of ligation of the left renal vein in resection of the abdominal aortic aneurysm. Surg Gynecol Obstet 1991;173:33–6.
13. Calligaro KD, Savarese RP, McCombs PR, et al. Division of the left renal vein during aortic surgery. Am J Surg 1990;160:192–6.
14. derrick jr, van rae, blocker tg. Constriction of the renal VEIN–A new concept in renal hypertension. Ann Surg 1964;160:589–95.
15. Shimada S, Hirose T, Takahashi C, et al. Pathophysiological and molecular mechanisms involved in renal congestion in a novel rat model. Sci Rep 2018;8:16808.
16. Vernon MA, Mylonas KJ, Hughes J. Macrophages and renal fibrosis. Semin Nephrol 2010;30:302–17.
17. Baptista-Silva JC, Dolnikoff MS, Moura LA, et al. Ligation of the left renal vein in epm1-Wistar rats: functional and morphologic alterations in the kidneys, testes and suprarenal glands. Sao Paulo Med J 1997;115:1475–84.
18. Breau RH, Clark E, Bruner B, et al. A simple method to estimate renal volume from computed tomography. Can Urol Assoc J 2013;7:189–92.
19. Korkmaz M, Aras B, Güneyli S, et al. Clinical significance of renal cortical thickness in patients with chronic kidney disease. Ultrasonography 2018;37:50–4.
20. Yamashita SR, von Atzingen AC, Iared W, et al. Value of renal cortical thickness as a predictor of renal function impairment in chronic renal disease patients. Radiol Bras 2015;48:12–6.
21. O'Neill WC. Sonographic evaluation of renal failure. Am J Kidney Dis 2000;35:1021–38.
22. Lam CF, Croatt AJ, Richardson DM, et al. Heart failure increases protein expression and enzymatic activity of heme oxygenase-1 in the lung. Cardiovasc Res 2005;65:203–10.
23. Shahid F, Lip GYH, Shantsila E. Role of monocytes in heart failure and atrial fibrillation. J Am Heart Assoc 2018;7:e007849.
24. Pappas L, Filippatos G. Pulmonary congestion in acute heart failure: from hemodynamics to lung injury and barrier dysfunction. Rev Esp Cardiol 2011;64:735–8.
25. Fortea JI, Puente Á, Cuadrado A, et al. Congestive hepatopathy. Int J Mol Sci 2020;21:9420.
26. Wang C, Ma C, Gong L, et al. Macrophage polarization and its role in liver disease. Front Immunol 2021;12:803037.

27. Tanaka S, Matsumoto T, Matsubara Y, et al. BubR1 insufficiency results in decreased macrophage proliferation and attenuated atherogenesis in apolipoprotein E-deficient mice. J Am Heart Assoc 2016;24:e004081.
28. Matsubara Y, Kiwan G, Liu J, et al. Inhibition of T-cells by cyclosporine A reduces macrophage accumulation to regulate venous adaptive remodeling and increase arteriovenous fistula maturation. Arterioscler Thromb Vasc Biol 2021;41:e160–74.
29. Kinoshita F, Tagawa T, Akamine T, et al. Interleukin-38 promotes tumor growth through regulation of CD8+ tumor-infiltrating lymphocytes in lung cancer tumor microenvironment. Cancer Immunol Immunother 2021;70:123–35.
30. Iseda N, Itoh S, Yoshizumi T, et al. ARID1A deficiency is associated with high programmed death ligand 1 expression in hepatocellular carcinoma. Hepatol Commun 2020;5:675–88.
31. Sugimoto M, Takahashi N, Niimi K, et al. Effect of intraoperative division of the left renal vein on the fate of renal function and left renal volume after open repair of para- and juxtarenal aortic aneurysm. Circ J 2019;83:1844–50.
32. Matsuo S, Imai E, Horio M, et al. Collaborators developing the Japanese equation for estimated GFR. Revised equations for estimated GFR from serum creatinine in Japan. Am J Kidney Dis 2009;53:982–92.
33. Bellomo R, Kellum JA, Ronco C. Defining and classifying acute renal failure: from advocacy to consensus and validation of the RIFLE criteria. Intensive Care Med 2007;33:409–13.
34. Baek JH. The impact of versatile macrophage functions on acute kidney injury and its outcomes. Front Physiol 2019;10:1016.
35. Le Clef N, Verhulst A, D'Haese PC, et al. Unilateral renal ischemia-reperfusion as a robust model for acute to chronic kidney injury in mice. PLoS One 2016;11:e0152153.
36. Wang YY, Jiang H, Pan J, et al. Macrophage-to-Myofibroblast transition contributes to interstitial fibrosis in chronic renal allograft injury. J Am Soc Nephrol 2017;28:2053–67.
37. Murray PJ, Wynn TA. Protective and pathogenic functions of macrophage subsets. Nat Rev Immunol 2011;11:723–37.
38. Wang X, Chen J, Xu J, et al. The role of macrophages in kidney fibrosis. Front Physiol 2021;12:705838.
39. Ross EA. Congestive renal failure: the pathophysiology and treatment of renal venous hypertension. J Card Fail 2012;18:930–8.
40. Diaz JA, Farris DM, Wrobleski SK, et al. Inferior vena cava branch variations in C57BL/6 mice have an impact on thrombus size in an IVC ligation (stasis) model. J Thromb Haemost 2015;13:660–4.